SAND2019-14833C

Multilevel Uncertainty Quantification Using CFD and OpenFAST Simulations of the SWiFT Facility

Alan Hsieh[1], David Maniaci[2], Thomas Herges[2], Gianluca Geraci[3], D. Thomas Seidl[3] and Michael Eldred[4]
Sandia National Laboratories, Albuquerque, NM, 87185, USA

Myra L. Blaylock[5] and Brent Houchens[5]
Sandia National Laboratories, Livermore, CA, 94550, USA

Uncertainty is present in all wind energy problems of interest, but quantifying its impact for wind energy research, design, and analysis applications often requires the collection of large ensembles of numerical simulations. For practical use these predictions require a range of model fidelity, as predictive models that include the interaction of atmospheric and wind turbine wake physics can require weeks or months to solve on institutional high-performance computing systems. The need for these extremely expensive numerical simulations exacerbate the computational resource requirements usually associated with uncertainty quantification analysis. To alleviate the computational burden, we propose here to adopt several multilevel-multifidelity strategies that we compare for a realistic test case. A demonstration study was completed using simulations of a V27 turbine at Sandia National Laboratories' SWiFT facility in a neutral atmospheric boundary layer. The flow was simulated with three models of disparate fidelity. OpenFAST with TurbSim was used stand-alone as the most computationally-efficient, lower-fidelity model. The computational fluid dynamics code Nalu-Wind was used for large-eddy simulations with both medium-fidelity actuator disk and high-fidelity actuator line models, with various mesh resolutions. In a pilot uncertainty quantification study, we considered five different turbine properties as random parameters: yaw offset, generator torque constant, collective blade pitch, gearbox efficiency and blade mass. The standard deviation of the estimated value for these properties decreases with the use of multilevel-multifidelity techniques compared to using a standard Monte Carlo method, and the amount of the improvement changes with the parameter being investigated.

I. Nomenclature

ABL	=	atmospheric boundary layer
AD	=	actuator disk
AL	=	actuator line
CV	=	control variate
CFD	=	computational fluid dynamics
f_i	=	body force
LES	=	large eddy simulation
MC	=	Monte Carlo

[1] Postdoctoral Appointee, Wind Energy Technologies Department.
[2] Senior Member of the Technical Staff, Wind Energy Technologies Department
[3] Senior Member of the Technical Staff, Optimization and UQ.
[4] Distinguished Member of the Technical Staff, Optimization and UQ.
[5] Principal Member of the Technical Staff, Thermal/Fluid Science & Engineering
.

MLMC = Multilevel Monte Carlo
MLMF = multilevel multifidelity
QoI = quantity of interest
SWiFT = Scaled Wind Farm Technology
UQ = uncertainty quantification

II. Introduction

In a typical wind farm, wind turbines may be placed in multiple rows in order to maintain a compact arrangement. The result of this arrangement is that the front rows of turbines will create a wake from the oncoming wind that will propagate to the wind turbines in back rows. The velocity deficit in these wakes tends to reduce the output power from those turbines, and hence the net wind farm efficiency may be lower than predicted from the nominal efficiency of a single turbine. The Scaled Wind Farm Technology (SWiFT) facility was designed and built to study these wake interactions, so it is an excellent resource for testing and validating methods to characterize wake effects [1].

A. Motivation

The wind industry engineering research and design practices are starting to use the tool of uncertainty quantification coupled with complex high-fidelity simulations. However, with the large number of uncertainty parameters, the computational cost becomes prohibitive for conventional UQ methods.

It is possible to use computational models to optimize the arrangement of wind turbines to minimize the loss of efficiency from the wake effects. However, models that do not consider variability in the operating conditions of the wind farm may lead to poor wind farm configurations; an optimally designed wind farm under a single nominal set of operating conditions offers no performance guarantees if the conditions deviate on any given day. Even when the turbine is operating within ideal conditions, the generated power is affected by turbulent fluctuations in the wind, changes in the wind shear and veer, atmospheric conditions such as density and stability, and the wakes from other turbines. Within the turbine itself, there may be misalignment with the primary wind direction, suboptimal blade pitch angles, and mis-tuned tolerances for the rotor and blade controllers. Finally, computational models for wind farms often rely on low order models that cannot capture all of the physics present in the system, and thus add model form uncertainty to the design of such systems.

Uncertainty quantification (UQ) is necessary for treating variability in applications whenever significant randomness in the system is present. In wind energy applications, UQ provides the ability to quantify the expected power output and associated variance from wind farms in the face of the aforementioned uncertainties in operating conditions. UQ may also be used to inform and optimize wind farm configurations that are robust to these variations and may yield superior performance to configurations designed without taking variability into account. Combining UQ methods with the extensive data taken at the SWiFT facility gives us the opportunity to test these methods against real research scale turbine measurements.

B. Multifidelity UQ

In recent years, multifidelity UQ has been introduced in order to alleviate the high computational cost of high-fidelity simulations for accurate wind simulations and it is based on the aggregation of several lower accuracy models with a handful of higher fidelity computations. This family of methods comprises both surrogate- and sampling-based approaches [2]. In this work, we focus our attention to sampling-based approaches but we leave the extension of surrogate-based multifidelity UQ strategies to a following paper. In the MLMC method the goal is to obtain a statistical estimator based on the aggregation of evaluations of the quantity of interest (QoI) over several model fidelities (very often spatial and temporal resolutions). MLMC takes advantage of the convergence of the deterministic scheme in order to build estimators that target the coarsest resolution levels and all the subsequent discrepancies between adjacent resolutions. The MLMC is based on the assumption that for a sequence of models, it is possible to build corrections with respect to the coarsest model and that these corrections exhibit a decreasing variance for increasing fidelity/resolution. In many practical circumstances, these assumptions are not always verified and it is necessary to resort to the so-called multifidelity estimators which are derived from the control variate approach [3, 4, 5]. The combination of control variate and MLMC lead to Multilevel-Multifidelity estimators (MLMF) [2]. As an extension of previous work [6], we consider simulations of Sandia National Laboratories' Scaled Wind Farm Technology (SWiFT) site in a neutral atmospheric boundary layer.

The turbulent wind is modeled with either Nalu-Wind [7] or TurbSim [8]. The latter is a large eddy simulation computational fluid dynamics (CFD) code. Both are coupled to OpenFAST (TurbSim being a package thereof) [9] which contains the turbine model.

Nalu-Wind simulations of the SWiFT site are part of an ongoing full-system (atmosphere, turbine and wake) validation effort of wind plant simulations named the SWiFT benchmarks [10, 11]. Within the study, numerous computational models of varying fidelity levels are subjected to comparisons with experimental observations from the SWiFT facility for three benchmarks of increasing levels of atmospheric stratification complexity: near neutral, slightly unstable and very stable. These model-measurement comparisons aim to reduce wind plant model uncertainty through assessment of model performance under different inflow conditions and model ability to reproduce mean and dynamic wake characteristics. For neutral atmospheric boundary layer operating conditions, Nalu-Wind was also used to simulate different yaw configurations for the upwind turbine, and the simulated inflow, loads and wake of the two turbines were compared to experimental wake steering results from the SWiFT facility [12]. Reasonable agreement was shown between the predicted inflow conditions, upwind turbine loads and the wake deficit with the measurement data.

III. Problem Description

A. SWiFT Experimental Site

Sandia National Laboratories operates the SWiFT facility located in Lubbock, Texas. The baseline site instrumentation includes three research wind turbines (WTG) and two meteorological towers (MET) as shown in Figure 1(a). The layout of the SWiFT facility is seen from an overhead view in Figure 1(b). The SWiFT turbines are highly-modified, variable speed collective pitch Vestas V27 machines with a hub height of 32.1 meters, a rotor diameter of 27 m, and a maximum power output of 192 kW [1]. The wind turbine (WTGa1) and meteorological tower (METa1) used to create these simulations are aligned with the predominant, southerly wind direction at the site. The wind turbines are highly instrumented with measurements including yaw heading, blade pitch angle, rotor rpm and azimuth angle in addition to generator power, torque, and rpm. The wind turbine yaw heading was calculated by subtracting the 32 m sonic anemometer wind direction from the wind turbine yaw heading. During the experimental campaign of focus in this paper, the Danish Technical University's (DTU) SpinnerLidar was deployed to measure the wake behind the upstream wind turbine [13]. Additional details about the neutral atmospheric inflow are included in Ref. [10] and details about the OpenFAST model calibration are provided in Ref. [11].

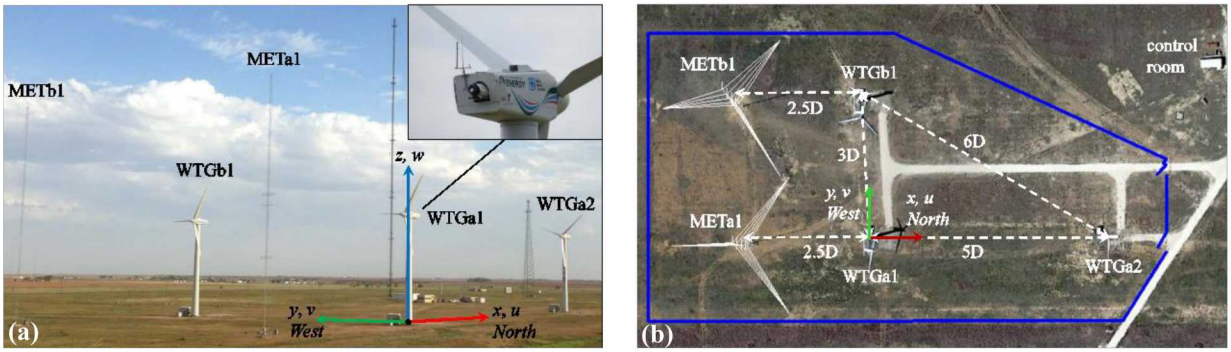

Figure 1. (a) SWiFT site layout and coordinate system with the DTU SpinnerLidar installed in WTGa1 (b) including a top view of the facility layout [1], where D = 27 m.

B. Multilevel Multifidelity Modeling Methodology

In this section we briefly describe the sampling approaches used for the UQ forward propagation in this paper, namely multilevel Monte Carlo (MLMC), control variate, and the multilevel-multifidelity (MLMF) estimator which combine the previous two approaches. All these estimators are derived from the Monte Carlo methods and therefore they exhibit an intrinsic variance, i.e. if the estimator is repeated multiple times different results are obtained. All the multilevel and/or multifidelity estimators aim at leveraging the computational efficiency of the less accurate models in order to reduce the variance of the statistical estimator built upon the highest fidelity model. In this context we consider the bias of the highest fidelity model, i.e. the LES Nalu-Wind code with actuator line for the fine mesh resolution, as satisfactory and therefore we only focus on the variance reduction aspect.

In a plain MC method the expected value $\mathbb{E}[Q]$ for a generic Quantity of Interest (QoI) $Q : \Xi \longrightarrow \mathbb{R}$ is approximated as

$$\mathbb{E}[Q] = \int_{\Xi} Q(\xi)\, p(\xi) d\xi \approx \hat{Q}_N^{MC} = \frac{1}{N}\sum_{i=1}^{N} Q\left(\xi^{(i)}\right) = \frac{1}{N}\sum_{i=1}^{N} Q^{(i)} \tag{1}$$

where N realizations of the vector of random input $\xi \in \mathbb{R}^d$ are drawn according to the joint probability distribution $p(\xi)$. For each realization of the vector of random input variable ξ, the value of the QoI $Q^{(i)} = Q(\xi^i)$ is computed by solving the system of PDEs describing the problem of interest. The MC estimator is robust and reliable, being unbiased and not affected by the dimensionality d, however its rate of convergence is only $\mathcal{O}(N^{\frac{1}{2}})$.

The first approach we investigate to reduce MC variance while keeping its cost affordable is the so-called MLMC. For a deep review of the method the interested reader can refer to [14]. The main idea of MLMC is to replace the QoI Q with a sequence of corrections with respect to a lesser accurate model (for instance, coarser spatial mesh resolutions). If we consider the highest resolution level Q_L we can write $Q_L = Q_0 + (Q_1 - Q_0) + \cdots + (Q_L - Q_{L-1})$ and if we define

$$Y_l = \begin{cases} Q_l - Q_{l-1} \text{ for } l > 0 \\ Q_0 \text{ for } l = 0 \end{cases} \tag{2}$$

we can write more compactly $Q_L = \sum_{l=0}^{L} Y_l$ The MLMC estimator is formulated by obtaining the expected value $\mathbb{E}[Q_L]$ as the sum of independent MC estimators for each term Y_l.

$$\hat{Q}_L^{MLMC} = \sum_{l=0}^{L} \frac{1}{N_l} \sum_{i=1}^{N_l} Y_l^{(i)}. \tag{3}$$

The variance of this estimator is known analytically once the terms $\mathbb{V}ar(Y_l)$ are estimated. Another notable feature of this method is that the sample allocation, i.e. the number of evaluations for estimating each term Y_l, can be obtained by solving an optimization problem in which a target accuracy ε^2 is prescribed and the overall computational cost, $C = \sum_{l=0}^{L} C_l N_l$, is minimized. If the cost of each realization of Y_l is noted as C_l the optimal solution is given by

$$N_l = \frac{1}{\varepsilon^2} \sum_{k=0}^{L} \sqrt{\mathbb{V}ar(Y_k) C_k} \sqrt{\frac{\mathbb{V}ar(Y_l)}{C_l}} \tag{4}$$

As it can be seen from the previous equation the number of simulations for each level is proportional to $\sqrt{\frac{\mathbb{V}ar(Y_l)}{C_l}}$. Therefore, for a sequence of levels for which $Y_l \to 0$ for $l \to \infty$, N_l will decrease as well with l, i.e. the computational burden is redistributed toward the less expensive coarser levels.

If the maximum number of available simulations at the highest resolution is fixed, i.e. $N_L = N_{target}$, the sample profile can be obtained by building backward the sequence of samples per each level as

$$\tau_{l-1} = \frac{N_l}{N_{l-1}} = \sqrt{\frac{\mathbb{V}ar(Y_l)}{C_l}} \sqrt{\frac{C_{l-1}}{\mathbb{V}ar(Y_{l-1})}} \; for \; l = L, \ldots, 1 \tag{5}$$

from which it follows that $N_{l-1} = N_l \tau_{l-1}$

In this work we explore the possibility to fuse realizations from Nalu-Wind and from OpenFAST. In general, whenever there is not a guarantee that $Y_l \to 0$ for $l \to 0$ (in our case statistics from OpenFAST will not likely converge to the statistics of Nalu-Wind), it is possible to rely on the so-called control variate (CV) estimator. The idea is to rely on the correlation among models instead of the decaying of variance among discrepancy terms. We briefly present a formulation in which the statistical properties of the high- and low-fidelity model (HF and LF respectively) are estimated as introduced in [2, 15]. Also, for an extension to multiple low-fidelity models, the reader can refer to [5, 16]. In the CV approach we can approximate the expected value of a QoI for the high-fidelity model evaluated at the resolution level $L(Q_L^{HF})$ by adding an unbiased term based on the low-fidelity model

$$\mathbb{E}[Q_L^{HF}] \approx \hat{Q}_{L,N_{HF}}^{CV,HF} = \hat{Q}_{L,N_{HF}}^{MC,HF} + \alpha\left(\hat{Q}_{L,N_{HF}}^{MC,LF} - \hat{Q}_{L,N_{LF}}^{MC,LF}\right), \tag{6}$$

where $N_{LF} = N_{HF} + \Delta_{LF} = N_{HF}(1 + r)$ and the additional LF evaluation $\Delta_{LF} = rN_{HF}$ are drawn independently from the first set N_{HF}. The values for α and the additional parameter r > 0 are obtained by minimizing the overall computational cost under the constraint of the variance of the estimator $\mathbb{V}ar(\hat{Q}_{L,N_{HF}}^{MC,HF})$ being equal to ε^2. The final result obtained through the optimization (see [2, 15] for further details)

$$N_{HF} = \frac{\mathbb{V}ar(Q_L^{HF})}{\varepsilon^2}\left(1 - \frac{r}{r+1}\rho^2\right) \text{and } r = -1 + \sqrt{\frac{C_{HF}}{C_{LF}}\frac{\rho^2}{1-\rho^2}}, \tag{7}$$

where ρ is the Pearson's correlation coefficient between HF and LF and C_{HF} and C_{LF} the computational cost of each HF and LF, respectively.

Instead of relying directly on the CV estimator, in this work we embed it within the MLMC estimator as done in [2, 6, 15, 17]. The MLMC estimator is obtained as in Eq.(3) and afterward for its coarsest level the MC estimator is replaced by a control, Eq.(6). The final result is similar to the MLMC allocation, with the sole difference that a variance reduction term Λ_l is introduced for $l = 0, i.e. \Lambda_0 = 1 - \frac{\rho_0^2 r_0}{1+r_0}$. If for all other levels $\Lambda_l = 1$ (which indicates that no variance reduction is achieved since there is not a CV at that level) the final sample allocation is

$$N_l = \frac{1}{\varepsilon^2} \sum_{k=0}^{L} \sqrt{\mathbb{V}ar(Y_k) C_k^{eq} \Lambda_k} \sqrt{\frac{\mathbb{V}ar(Y_l)\Lambda_l}{C_l^{eq}}} \tag{8}$$

where the equivalent cost per each level l also includes the additional number $r_l N_l^{HF}$ of low-fidelity evaluations, $C_l^{eq} = C_l^{HF} + (1 + r_l) C_l^{LF}$.

For this estimator we can also compute the ratios τ_l similarly to Eq. (5) in order to build the optimal allocation constrained to the maximum number of realizations at the highest level of resolution of the HF model.

IV. Various Fidelity Computational Turbulence Sub-Models

Various approaches are employed here to simulate the single leading Vestas V27 wind turbine (WTGa1) used at SWiFT [13]. The various fidelity sub-models include two models for the inflow and multiple strategies to couple the turbine to the flow field. The inflow wind for the aerodynamic analysis is simulated either using the highly efficient TurbSim or the high-resolution Nalu-Wind LES code.

Independent of the turbulence model, the modeling of the wind turbine loads is through the OpenFAST software suite developed at the National Renewable Energy Laboratory (NREL) [9]. OpenFAST enables the analysis of complex physical and environment coupling, including turbine controllers, elastic dynamics, and flow-structure interactions with actuator line and disk theory. The Vestas V27 [1] model in OpenFAST is used to match the rotors used at SWiFT.

A summary of the four simulation model levels is shown in Table 1. The OpenFAST modular time step was kept constant at 0.005 seconds for all models; Table 1 displays the time step of the atmospheric model (Nalu-Wind or TurbSim). Mesh information is not included for TurbSim as the mesh does not have the same meaning as the Nalu-Wind CFD mesh.

Table 1: Case Descriptions for Simulation Models

Case	Grid Number (# elements)	Min. Grid Spacing (m)	Domain (x,y,z) (km)	Sim. Time Step (s)
OpenFAST + TurbSim	-	-	-	0.05
Nalu-Wind + AD coarse	9.5e6	2.5	3 x 3 x 1	0.2
Nalu-Wind + AD fine	11.7e6	1.25	3 x 3 x 1	0.2
Nalu-Wind + AL fine	11.7e6	1.25	3 x 3 x 1	0.02

A. OpenFAST and TurbSim Alone

The most computationally affordable modeling method is to use the OpenFAST module TurbSim to generate statistical realizations of a turbulent inflow wind field combined with the AeroDyn module for solving the turbine rotor aerodynamic loads. This method is the lower fidelity modeling approach and is termed OpenFAST in this paper, despite the use of some OpenFAST modules in the Nalu-Wind code. TurbSim models the turbulent inflow based on a statistical representation where the spatiotemporal turbulent velocity field relationships are enforced, in this case the Kaimal spectra [8]. Many inflow parameters can be varied in TurbSim, such as shear, turbulence intensity, and mean wind speed, but these parameters cannot all be enforced in the same way in Nalu-Wind LES. The present work only focuses on varying turbine parameters, and future work will focus on inflow and atmospheric boundary layer

parameters. AeroDyn uses the blade element momentum theory and general actuator disk methods to model the aerodynamic loads on a wind turbine rotor, and a major limit of this method is that it does not capture wake interaction, and so only applies to stand alone wind turbines.

B. Nalu-Wind with OpenFAST Coupling

The second set of methods employ the Large Eddy Simulations (LES) capabilities of the massively parallel simulation code Nalu-Wind [7] in conjunction with turbine forcing models from OpenFAST. Nalu-Wind solves the integral forms of conservation of mass

$$\int \frac{\partial \bar{\rho}}{\partial t}\, dV + \int \bar{\rho}\tilde{u}_i n_i\, dS = 0 \tag{9}$$

and momentum

$$\int \frac{\partial \bar{\rho}\tilde{u}_i}{\partial t}\,\mathrm{d}V + \int \bar{\rho}\tilde{u}_i\tilde{u}_j n_j\,\mathrm{d}S = \int \tilde{\sigma}_{ij} n_j \mathrm{d}S - \int \tau_{ij}^{sgs} n_j \mathrm{d}S + \int (\bar{\rho} - \rho_\circ) g_i \mathrm{d}V \tag{10}$$

in the low-Mach number limit. The tilde represents Favre averaging (quantities weighted by instantaneous density before averaging). A one-equation, constant coefficient, turbulent kinetic energy model is used for the subgrid scale stresses [18].

There are two steps to modeling a wind turbine in a neutral atmospheric boundary layer (ABL) flow using Nalu-Wind. First just the ABL is established, then either Actuator Disk (AD) or Actuator Line (AL) turbine models are added. The AD and AL are implemented by coupling Nalu-Wind with OpenFAST, which uses the blade element method to compute turbine loads as well as handling turbine dynamics and controls.

The ABL is setup by running on a 10 m resolution mesh for 20,000 seconds with the flow along the *x*-axis and the *z*-axis pointing upwards. The inflow/outflow planes are periodic, and sides parallel to the wind flow are also periodic. The upper boundary is represented by an inviscid wall with a specified temperature gradient that matches the gradient above the capping inversion. The ground is represented by a wall boundary condition with a roughness factor of 0.01. The velocity is set to 8.69 m/s at the hub height of 32.1m off the ground, and the velocity profile is allowed to develop with that constraint. After the fully turbulent flow has been established in the first 20,000 s, the simulation is run for an additional 630 s. (The first 30 s of this will be discarded so that the start-up effects of the turbine will not be used in the statistics for the quantities of interest.) During this time the velocity data on the inflow/outflow plane is saved.

In the next step this velocity data is used as the inflow for 630 s of simulation with an AL or AD model running. The initial condition is set to be the flow field in the entire domain at 20,000 s, so it is in sync with the initial inflow velocity. For these runs the meshes have a refined area around the turbine. Two refinement levels are used in this study. For the first (coarse, "C") mesh, there is a refinement region that halves the spacing from 10 m to 5 m in an area 540 x 140 x 100 m, staring 190 m in front of the turbine and a region inside that where the spacing is reduce to 2.5 m which is 520 x 120 x 90 m, starting 180 m in front of the turbine. For the next mesh (designated as fine, or "F" in the results section), another refinement region with a spacing of 1.25 is added inside the other two that is 500 x 100 x 80 m and 170m in front of the turbine. These refinement zones are shown in Fig 1.

In between each of the refinement zones, there is a thin (the width of the larger spacing of the two regions it is in between) region of tetrahedron and hexahedron shaped elements to allow for the reduction in the spacing. The sizes of these meshes are described in Table 1.

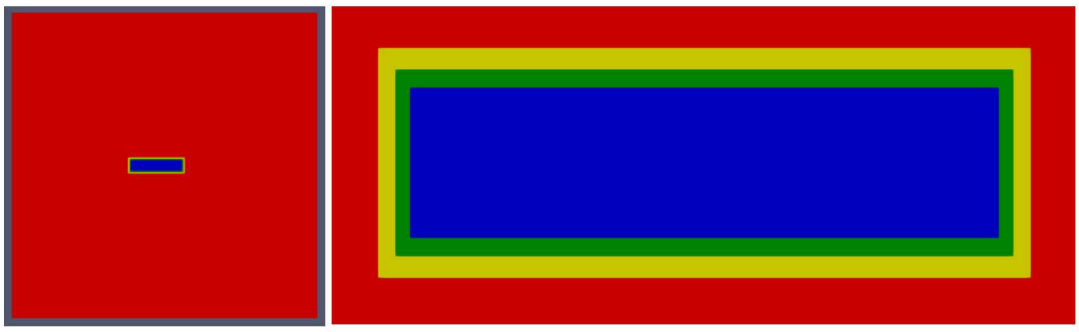

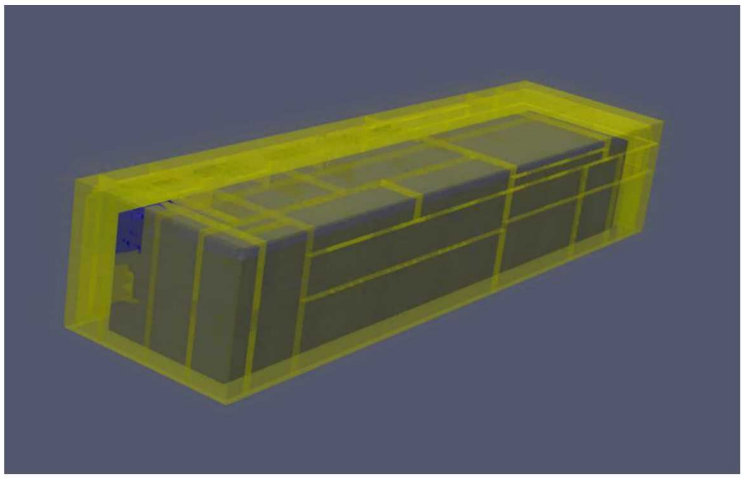

Figure 2 Top left: Bottom view of the entire mesh. The area in red shows where the spacing is 10 m, and the other colors show the refinement regions. Top right: Shows a closer look at the refinement regions. The yellow region has a spacing of 5 m for all grids. For the coarsest grid, the green and blue regions all have a spacing of 2.5 m. For the fine grid, the blue region has a spacing of 1.25 m. Bottom: To give a perspective of the relative heights of the refinement regions, the 5 m spacing region is shown in transparent yellow; the finest spacing of 1.25 m is shown in blue. The rest of the mesh (not shown) continues 910 m above the yellow region.

In Nalu-Wind, the wind turbine rotor and tower may be modeled using actuator source representations, such as actuator lines and actuator disks. In contrast to blade-resolved simulations in which the blade surfaces are modeled through complex fluid-structure interactions, actuator source representations do not resolve the blade boundary layer. However, actuator source modeling has been shown in previous studies to be competitive in accuracy with blade-resolved simulations and is far less computationally expensive [19].

C. Nalu-Wind with OpenFAST Actuator Disk Coupling

In the actuator disk model, the body-force is applied over the entire rotor disk at once, removing the blade-like discrete forces in the actuator line model [19]. Although the actuator disk does not accurately model flow features such as blade-local axial induction zones and root/tip vortices, the model has lower temporal and spatial resolution constraints than actuator line. The total actuator force at each discrete radial location is first computed,

$$F(r_j) = \sum_{i=1}^{N_B} f(r_j, \theta_j) \tag{11}$$

where $f(r_j, \theta_j)$ are the forces at each actuator line point. This total force is then spread evenly throughout the actuator line points in addition to swept points that are evenly distributed azimuthally. The disk-applied force $f(r_j)$,

$$f(r_j) = \frac{F(r_j)}{N_B(N_{S,j} + 1)} \tag{12}$$

is then spread across all points at a given radius r_j. N_B and $N_{S,j}$ refer to the number of blades and the number of swept points for a given radius.

D. Nalu-Wind with OpenFAST Actuator Line Coupling

The actuator line model represents the turbine blades as a body-force source term, f_i, computed from the forces over the actuator line [19]. To calculate the volumetric f_i, which is a force per unit volume, the non-volumetric actuator forces over the line F_i' requires projection into the fluid volume. Nalu-Wind uses the uniform Gaussian projection function proposed by Sorenson and Shen [20],

$$g(\vec{r}) = \frac{1}{\pi^{\frac{3}{2}}\varepsilon^3} e^{-\left(\frac{|\vec{r}|}{\varepsilon}\right)^2} \tag{13}$$

in which $\vec{r}$ is the position vector from the fluid location where the Gaussian is applied to an actuator line element control point, and ε is the spreading width of the Gaussian which determines the dilution of the body force. For an actuator line extending from $l = 0$ to L, the body force at (x,y,z) is represented as

$$f_i(x,y,z) = \int_0^L g\big(\vec{r}(l)\big)F_i'(l)dl. \tag{14}$$

This expression may be simplified when the actuator line is discretized into line elements,

$$f_i(x,y,z) = \sum_{k=0}^{N} g(\vec{r}^k)F_i^k. \tag{15}$$

where F_i^k, being the force computed at each element center and k being the actuator line index.

V. Results

A. Computational Costs of Various Sub-Models

Although the LES-based actuator line approach of Nalu-Wind is expected to be more accurate than the OpenFAST approach, the computational cost associated with solving the filtered Navier-Stokes equations on a large domain is substantially higher. Thus we compare the costs of performing an LES on two separate meshes with the AL and AD models versus the cost of using OpenFAST with TurbSim. All simulations were run for a total simulation time of 630 seconds.

Table 2 reports the relative simulation costs for running OpenFAST and for running Nalu-Wind on two meshes of varying resolution, referred to here as AD coarse, AD fine and AL coarse. The OpenFAST cost includes the amount of time required to generate the inflow turbulence realization using TurbSim, but even with this cost, it is orders of magnitude cheaper to run OpenFAST than even the coarse grid LES in Nalu-Wind. The four QoIs were the ten-minute means of generated power, total rotor thrust, flapwise blade-root bending moment and edgewise blade-root bending moment.

Table 2: Cost Estimates for Nalu-Wind and OpenFAST Simulations

Case	Simulation Time (hrs)	CPUs	Cost (CPU-hours)	Cost (relative)
OpenFAST + TurbSim	0.25	1	0.25	1
Nalu-Wind + AD coarse	7	768	5,376	21,504
Nalu-Wind + AD fine	16.5	768	12,672	50,688
Nalu-Wind + AL fine	31.75	768	24,384	97,536

For the present study, the OpenFAST and Nalu-Wind simulations were scheduled and run using the Dakota [21] uncertainty quantification toolkit developed by Sandia National Laboratories. Dakota provides a flexible, extensible interface between simulation codes such as Nalu-Wind and iterative analysis methods including but not limited to parameter estimation, sensitivity/variance analysis and uncertainty quantification with sampling, reliability and stochastic expansion methods. Dakota also provides parallel computing capabilities, which allows the Nalu-Wind simulations to be run on Sandia's high-performance capacity cluster systems using hundreds of processors.

B. Pilot Study

The following section describes the results of the sampling study for key quantities of interest from the turbine operations. The five aleatoric uncertain turbine parameters of interest were the yaw offset, generator torque constant, collective blade pitch, gear box efficiency and blade mass density scaling factor. These values were then mapped onto the respective intervals shown in Table 2 for the five input turbine parameters. These bounds were determined from observed V27 turbine operational data from the wake steering experiment at the SWiFT site.

Within the environment of OpenFAST, separate input files exist for each OpenFAST module. The yaw offset and gear box efficiency were modified using the 'NacYaw' and 'GBoxEff' variables in ElastoDyn, which models the turbine structural dynamics. The generator torque constant was modified using the 'VS_Rgn2K' variable in ServoDyn, which models the turbine control and electric drive dynamics. The collective blade pitch was modified using the

'BlPitch' and 'BlPitchF' variables in ElastoDyn and ServoDyn respectively, representing the initial and final blade pitches. The blade mass density scale factor was modified using the 'AdjBlMs' variable in the individual blade file that is read into ElastoDyn.

Table 2: Bounds of Input Turbine Variables

Input Variable	Units	Lower Bound	Upper Bound
Yaw Offset	(deg)	-25	25
Generator Torque Constant	(N-m/rpm^2)	0.0003	0.0004
Collective Blade Pitch	(deg)	-1.5	0
Gear Box Efficiency	(%)	90	100
Blade Mass Scale Factor	(-)	0.9	1.1

In Figure 3, the computed values for the four QoIs are displayed from the different Nalu-Wind and OpenFAST simulation levels. For all considered QoIs (power, thrust, loads), the Nalu simulations predict values ranging from ten to fifty percent higher than the corresponding OpenFAST simulations.

For both bending moment QoIs, the Nalu-AD results for the coarse and fine meshes are very similar for all samples but for generator power and thrust, discrepancies are observed between the two levels. Nalu-AL has a higher generated power and the two bending moments compared to the Nalu-AD simulations.

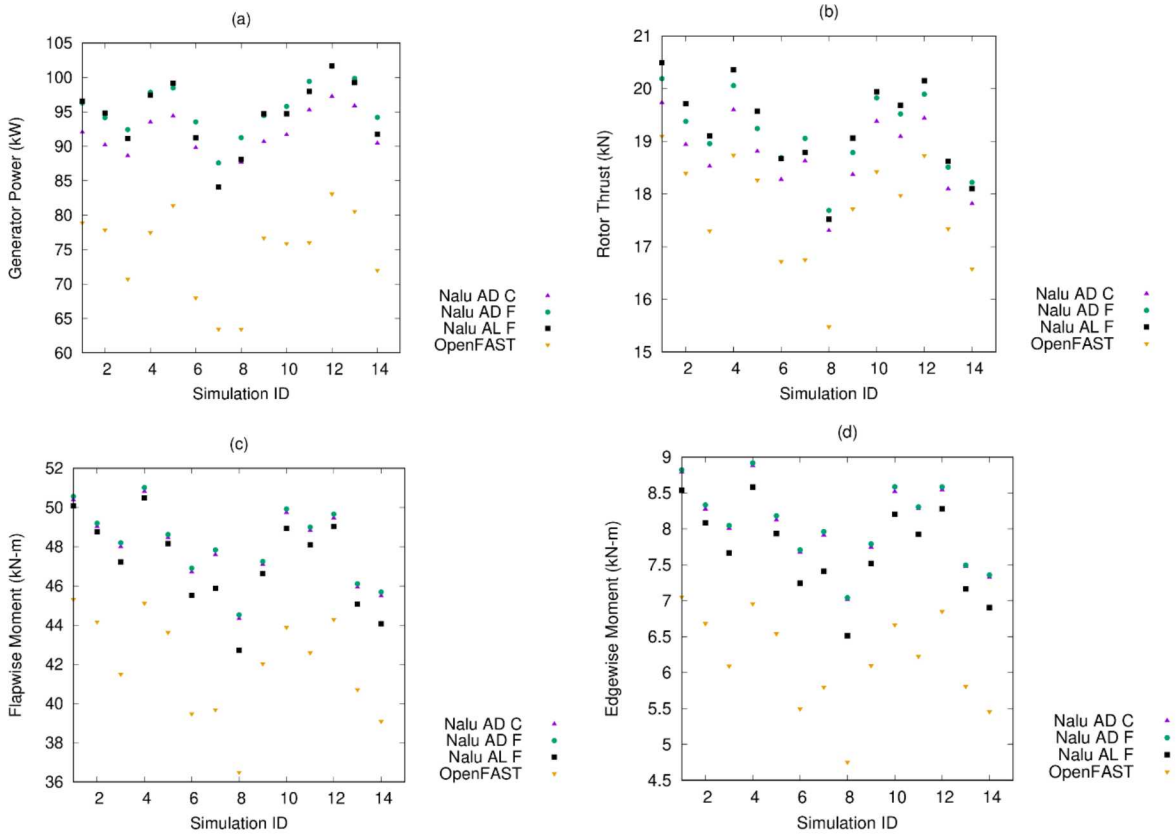

Figure 3. Computed values from the Nalu/OpenFAST simulations for a) generated power; b) rotor thrust; c) flapwise blade-root bending moment; d) edgewise blade-root bending moment. AD are the actuator disk simulations; AL are the actuator line; C designates the "coarse" mesh where "F" is the "fine" mesh.

In Figure 4, the multilevel corrections are shown between the different levels for the four considered QoIs. The decreases are non-monotonic due to the similarities between the Nalu-Wind actuator disk and actuator line models.

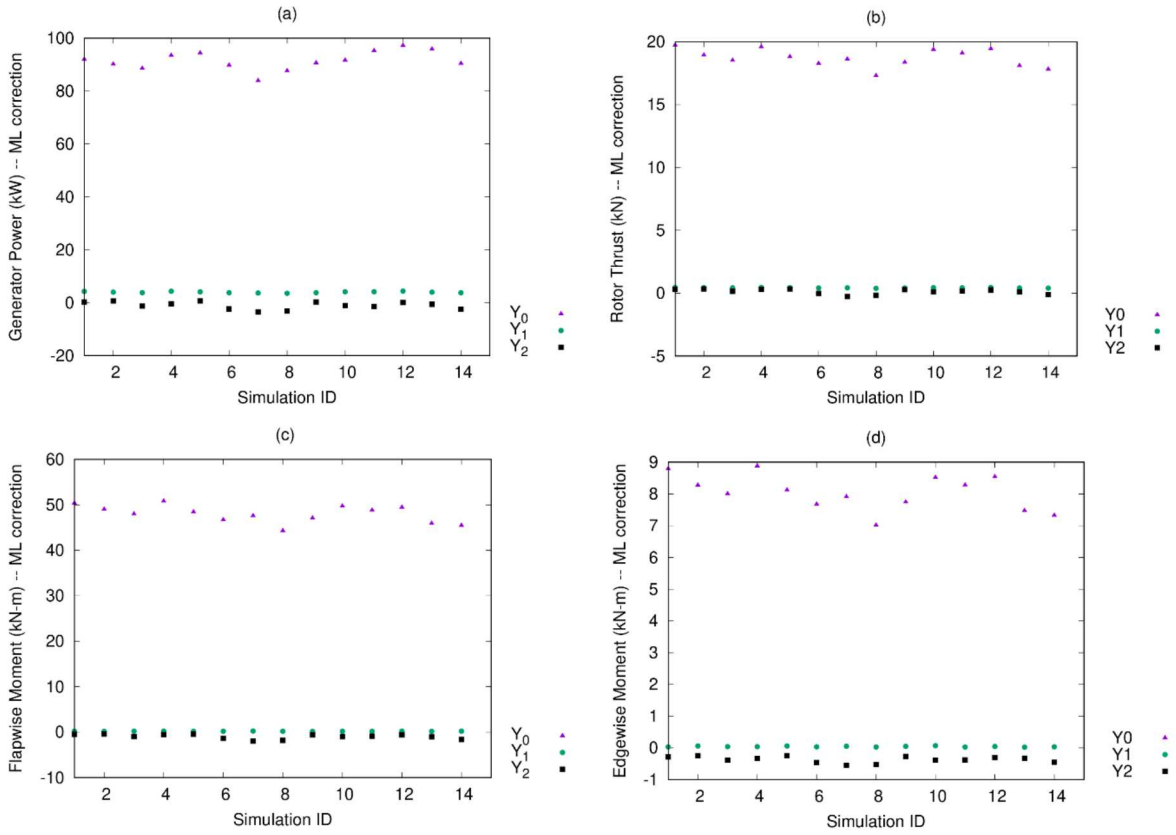

Figure 4. Multilevel corrections ($Y_l = Q_l - Q_{l-1}$) for a) generated power; b) rotor thrust; c) flapwise blade-root bending moment; d) edgewise blade-root bending moment.

Using the statistical properties derived from the results of the pilot study, we are able to extrapolate the behavior of several estimators:

- MC: Standard Monte-Carlo estimator;
- MLMC-3l: Multilevel $Q_0 + (Q_1 - Q_0) + (Q_2 - Q_1)$;
- MLMC-2l: Multilevel $Q_1 + (Q_2 - Q_1)$;
- MLMF-3l: MLMF based on MLMC-3l with CV for Q_0;
- MLMF-2l: MLMF based on MLMC-2l with CV for Q_1.

In Figure 5, the standard deviation for each estimator is shown as a function of the high-fidelity model simulations required to obtain the same result for the four different QoIs. A lower estimator standard deviation indicates better reliability for a particular sampling method. In Figure 5(b) for rotor thrust, the MC line overlaps with the MLMC-2l distribution.

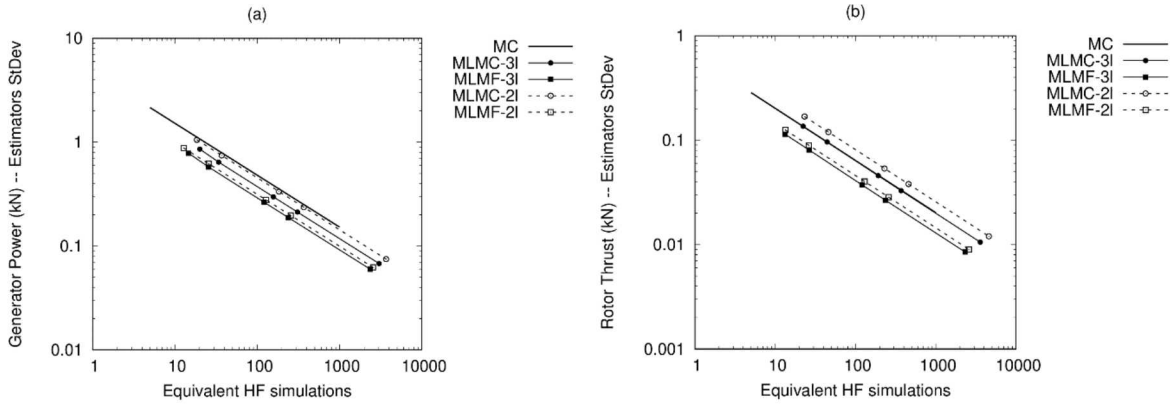

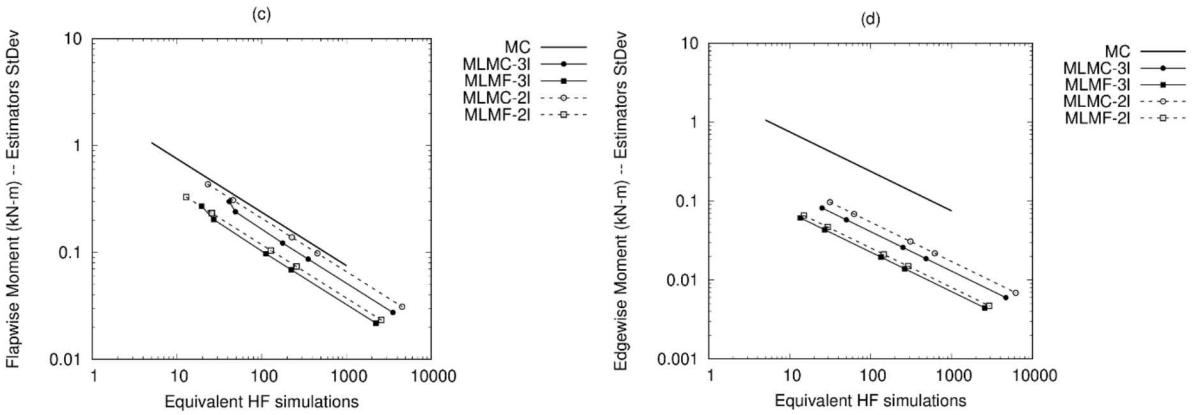

Figure 5. Extrapolated performance for the MC/MLMC/MLMF estimators for a) generated power; b) rotor thrust; c) flapwise blade-root bending moment; d) edgewise blade-root bending moment.

For all considered QoIs, the two most efficient estimators were MLMF-3l and MLMF-2l, with the former consistently showing the best performance. The results illustrate that MLMF sampling methods consistently reduce estimator variance regardless of QoI. The MLMC-3l and MLMC-2l performed similarly for all QoIs, however their performance in relation to MC and MLMF varied depending on the QoI. For edgewise blade-root bending moment in Figure 5(d), a significant improvement is observed for the MLMC methods over single-level Monte Carlo. For generator power in Figure 5(a), the improvement from MC to MLMC is small. For rotor thrust in Figure 5(b), single-level Monte Carlo shows equivalent efficiency to MLMC-3l and higher efficiency than MLMC-2l, demonstrating that MLMC does not necessarily have the consistent improvement over MC that MLMF methods possess.

VI. Conclusion

In this study, we compared several estimators: single-level Monte Carlo, multi-level Monte Carlo and multi-level multifidelity methods, for a wind turbine application using the physics models of TurbSim+OpenFAST and Nalu-Wind. The conducted Nalu-Wind simulations for the pilot study used a quasi-steady-state turbulent inflow of a neutral atmospheric boundary layer, providing detail of atmospheric-turbine interactions similar to benchmark simulations.

The performance of the estimators varied between four tested QoIs, with the MLMF approaches consistently requiring the fewest equivalent samples for a given level of accuracy. The MLMC methods performed similar to MLMF methods for generator power, but showed a significance decrease in efficiency for rotor thrust and bending moments. For rotor thrust, single-level MC showed equivalent efficiency to a third-level MC method, which can be attributed to the non-monotonic behavior of the different simulation model levels.

Acknowledgments

Sandia National Laboratories is a multimission laboratory managed and operated by National Technology & Engineering Solutions of Sandia, LLC, a wholly owned subsidiary of Honeywell International Inc., for the U.S. Department of Energy's National Nuclear Security Administration under contract DE-NA0003525. The views expressed in the article do not necessarily represent the views of the U.S. Department of Energy or the United States Government. This work was accomplished through funding from the U.S. Department of Energy Wind Energy Technology Office.

References

[1] J. Berg *et al.*, "Scaled Wind Farm Technology Facility Overview," in *AIAA SciTech 32nd Wind Energy Symposium*, 2014

[2] Geraci, G., Eldred, M., Gorodetsky, A. and Jakeman, J. "Recent advancements in Multilevel-Multifidelity techniques for forward UQ in the DARPA Sequoia project." *AIAA SciTech 2019 Forum*, 2019.

[3] L.W.T. Ng & K.E. Willcox "Multifidelity approaches for optimization under uncertainty." *Int. J. Numer. Meth. Engng*., vol. 100(10), pp. 746-772, 2014.

[4] Pasupathy, R., Taaffe, M., Schmeiser, B. W. & Wang, W. "Control-variate estimation using estimated control means." *IIE Transactions*, vol. 44(5), pp. 381-385, 2014.

[5] Peherstorfer, B., Willcox, K., Gunzburger, M. "Optimal model management for multifidelity Monte Carlo estimation." *SIAM Journal on Scientific Computing*, vol. 38(5), A3163A3194, 2016.

[6] Maniaci, D. and Frankel, A. and Geraci, G. and Blaylock, M. and Eldred, M. "Multilevel Uncertainty Quantification of a wind turbine large eddy simulation model." *7th European Conference on Computational Fluid Dynamics (ECFD 7)* 11-15 June 2018, Glasgow, UK, 2018.

[7] S. P. Domino, "Sierra Low Mach Module: Nalu Theory Manual 1.0. SAND2015-3107W," Sandia National Laboratories, Sandia National Laboratories Unclassified Unlimited Release (UUR)SAND2015-3107W, 2015, Available: https://github.com/NaluCFD/NaluDoc.

[8] "NWTC Information Portal (TurbSim)," ed. https://nwtc.nrel.gov/TurbSim. Last modified 5-Jan-2018; Accessed 04-December-2019

[9] "NWTC Information Portal (OpenFAST)," ed. https://nwtc.nrel.gov/OpenFAST. Last modified 14-June-2016; Accessed 05-December-2019

[10] P. Doubrawa *et al.*, "Benchmarks for Model Validation based on LiDAR Wake Measurements," *Journal of Physics: Conference Series,* vol. 1256, p. 012024, 2019/07 2019.

[11] P. Doubrawa *et al.*, "Modeling wind turbine wakes in stratified conditions: the SWiFT model validation benchmarks," *Soon to be published,* 2020.

[12] M. L. Blaylock, B. Houchens, D. C. Maniaci, T. G. Herges, A. S. Hsieh, R. C. Knaus and P. Sakievich, "Comparison of Field Measurements and Large Eddy Simulations of the Scaled Wind Farm Technology (SWiFT) Site," presented at the Proceedings of the ASME-JSME-KSME 2019 Joint Fluids Engineering Conference, 2019.

[13] T. G. Herges, D. C. Maniaci, B. T. Naughton, T. Mikkelsen, and M. Sjöholm, "High resolution wind turbine wake measurements with a scanning lidar," presented at the Wake Conference 2017, 2017.

[14] M. B. Giles, "Multi-level Monte Carlo path simulation," *Oper. Res.,* vol. 56, pp. 607-617, 2008.

[15] Gorodetsky, A. and Geraci, G. and Eldred, M. and Jakeman, J. "A Generalized Approximate Control Variate Framework for Multifidelity Uncertainty Quantification." arXiv preprint arXiv:1811.04988v3, 2018.

[16] Geraci, G. and Eldred, M. and Iaccarino, G. "A multifidelity control variate approach for the multilevel Monte Carlo technique." *CTR Annu. Res. Briefs*. pp. 169-181, 2015.

[17] Fairbanks, H. and Doostan, A. and Ketelsen, C. and Iaccarino, G. "A low-rank control variate for multilevel Monte Carlo simulation of high-dimensional uncertain systems." *Journal of Computational Physics*, vol. 341, pp. 121-139, 2017.

[18] A. Yoshizawa and K. Horiuti, "A statistically-derived subgrid-scale kinetic energy model for the large-eddy simulation of turbulent flows," *J. Phys. Soc. of Japan,* vol. 54, pp. 2834-2839, 1985.

[19] M. Churchfield, S. Shreck, L. A. Martinez-Tossas, C. Meneveau and P. R. Spalart, "An advanced actuator line method for wind energy applications and beyond," presented at AIAA SciTech 2017, 2017.

[20] J. N. Sorensen and W. Z. Shen, "Numerical modeling of wind turbine wakes," *Journal of Fluids Engineering,* vol. 124, no. 2, pp. 393-399, 2002.

[21] Adams, B.M., Bauman, L.E., Bohnho_, W.J., Dalbey, K.R., Ebeida, M.S., Eddy, J.P., Eldred, M.S., Geraci, G., Hooper, R.W., Hough, P.D., Hu, K.T., Jakeman, J.D., Maupin, K.A., Monschke, J.A., Rushdi, A., Swiler, L.P., Vigil, D.M, and Wildey, T.M., Dakota, A Multilevel Parallel Object-Oriented Framework for Design Optimization, Parameter Estimation, Uncertainty Quantification, and Sensitivity Analysis: Version 6.0 Users Manual. Sandia National Laboratories SAND2014-4633. Updated November 2016 (Version 6.5).